Journal of Industrial and Engineering Chemistry 72 (2019) 346–353

Contents lists available at ScienceDirect

Journal of Industrial and Engineering Chemistry

journal homepage: www.elsevier.com/locate/jiec

Enhanced filtration performance and anti-biofouling properties of antibacterial polyethersulfone membrane for fermentation broth concentration

Longbin Qi[a,b,c], Yunxia Hu[a,*], Qingzhi Chai[b], Qun Wang[a]

[a] State Key Laboratory of Separation Membranes and Membrane Processes, School of Materials Science and Engineering, Tianjin Polytechnic University, Tianjin 300387, PR China

[b] CAS Key Laboratory of Coastal Environmental Processes and Ecological Remediation, Yantai Institute of Coastal Zone Research, Chinese Academy of Sciences, Yantai, Shandong Province 264003, PR China

[c] University of Chinese Academy of Sciences, Beijing 100049, PR China

ARTICLE INFO

Article history:
Received 14 October 2018
Received in revised form 6 December 2018
Accepted 22 December 2018
Available online 28 December 2018

Keywords:
Fermentation broth
Biofouling mitigation
Membrane
Silver nanoparticles

ABSTRACT

The anti-biofouling performance of silver nanoparticles (Ag NPs) modified polyethersulfone (PES) membrane was evaluated during the concentration of fermentation broth. The Ag NPs containing membrane did not exhibit biofouling mitigation performance during the first filtration cycle, but could help to recover water flux upon physical cleaning. After three filtration-clean cycles, the Ag NPs containing membranes presented higher water flux and slower flux decline than the control membranes without Ag NPs. Ag NPs on the membrane surface facilitated the effective removal of cake layer. Moreover, the Ag NPs-containing membrane had no negative effects on the activities of bacteria in fermentation broth.

Introduction

Fermentation broth concentration is one of the required processes in industrial fermentation fields including pharmaceutical manufacturing, chemical engineering, food production, and others [1–4]. Membrane separation technology has been extensively used for industrial fermentation broth concentration due to its high separation efficiency, low operation cost, and continuous facile operation [5–7]. However, the complex components in the fermentation broth such as bacterial cells, bacteria secreted proteins and polysaccharide, and nutrient medium have strong negative effects on the membrane flux and the concentration efficiency [8–10]. Moreover, the microorganisms would form a thick cake layer on membrane surface and then develop into biofilms to block membrane pores resulting in the decreased membrane flux [8,11–13]. Therefore, the improvement of the membrane resistance against biofouling is highly desired to facilitate the extensive applications of membrane filtration technology for fermentation broth concentration.

Several strategies have been developed to mitigate membrane biofouling in the fermentation broth concentration including optimization of operation conditions [9,14,15], physical and chemical cleaning [16–18] and antibacterial membrane employment [19,20]. However, it is extremely difficult to remove the biofilm completely from the membrane surface through the optimization of operation conditions. Moreover, bacteria generally enter membrane pores and develop biofilm inside, which cause severe water flux decline [21,22]. Although strong chemicals and frequent cleaning operation can remove the biofilm inside membrane pores, they generally impair membrane structure and thus reduce the membrane performances in the long-term operation [23]. Fabrication of antibacterial membranes was considered as an effective method for membrane biofouling mitigation. The antibacterial materials can inactivate bacteria, decrease the secretion of extracellular polymeric substances, and inhibit the biofilm development [20,24]. Both releasable biocides (e.g., silver-based and copper-based nanomaterials) and unreleasable biocides (e.g., cationic polymeric materials, carbon nanotube and graphene-based nanomaterials) have been incorporated onto the membrane surfaces or matrix to alleviate membrane biofouling [25–30]. Among these, silver nanoparticles (Ag NPs) is one of the most widely used biocides due to their excellent antimicrobial properties and low toxicity to mammal

* Corresponding author.
E-mail addresses: yunxiahu@yic.ac.cn, yunxiahu@tjpu.edu.cn (Y. Hu).

https://doi.org/10.1016/j.jiec.2018.12.036
1226-086X/

cells [31–33]. Several strategies have been developed to fabricate Ag NPs loaded antibacterial membrane. For example, blending Ag NPs in casting solution to prepare antibacterial membranes through phase inversion is one of the commonly used approaches [34,35]. However, this approach embeds a very limited amount of Ag NPs on membrane surface. Grafting Ag NPs onto the membrane surface may increase Ag NPs numbers on membrane surface and enhance the interaction between Ag NPs and membrane through chemical bonding [36,37]. However, this approach needs to functionalize the Ag NPs or membrane surfaces, which is a complex process and is not convenient to scale up for real applications. Recently, we developed a simple method to in situ generate Ag NPs on the polydopamine modified polyamide membrane achieving the improved anti-biofouling performance [38–40]. The Ag NPs were uniformly distributed on the membrane surface with high loading amount and slow release.

Antibacterial membranes have been proven to exhibit great performances of mitigating biofouling and alleviating the membrane flux decline during water treatments, which is generally under mild biofouling conditions having less population of bacteria ($\sim 10^7$ CFU mL^{-1}) in the feed solution [35,41,42]. Under severe biofouling conditions with very dense population of bacteria and complex components in the fermentation broth, the thick cake layer of bacteria would be formed immediately on the membrane surface during the filtration process, and the membrane flux dropped down rapidly [8,13,43]. Very few work focused on the investigation of antibacterial membranes used for fermentation broth concentration. It is also challenging to predict the performances of antibacterial membranes under such severe biofouling conditions without experimental results [20]. Moreover, it is not clear yet but important to know the impact of antibacterial membranes on the activities of bacteria in the fermentation broth. Thus, it deserves a comprehensive investigation of the antibacterial membranes used for the fermentation broth concentration.

Herein, we fabricated silver nanoparticles (Ag NPs) containing polyethersulfone (PES) antibacterial microfiltration (MF) membranes and investigated their performances in the fermentation broth concentration. We adopted our previous protocol to in situ grow Ag NPs on the PES MF membranes via the polydopamine coating [38]. The impacts of Ag NPs generation on the membrane water permeability and surface hydrophilicity were investigated. The antibacterial properties of Ag NPs containing membranes were examined. Importantly, the water flux and flux recovery of Ag NPs containing membranes were monitored during the concentration of the simulated fermentation broth in a lab-scale cross-flow microfiltration system with a periodic back-washing operation. The cake layer formed on membrane surface was analyzed using confocal laser scanning microscope (CLSM) after the filtration and cleaning process. The stability of Ag NPs on the membrane surface and their influence on the bacteria activity were investigated. Our work also elucidated the biofouling mitigation mechanism of Ag NPs containing membranes during the fermentation broth concentration.

Experimental

Materials

A commercial PES MF membrane with an average pore size of 0.22 μm was obtained from American Membrane Corporation. Propidium iodide (PI) and dopamine were purchased from Sigma Aldrich (St. Louis, MO, USA). SYTO®9 was received from Invitrogen (Eugene, Oregon, USA). Tris–HCl buffer (1M, pH 8.5) was supplied by Beijing Solarbio Science & Technology Co., Ltd., China. *Escherichia coli* (*E. coli*, DH5α) were obtained from Beijing Dingguo Changsheng Biotechnology Co., Ltd., China. Luria-Bertani (LB) broth was purchased from Oxoid Limited, UK. Silver nitrate, sodium chloride, sodium bicarbonate and isopropanol were received from Sinopharm Chemical Reagent Beijing Co., Ltd., China.

Preparation of Ag NPs containing PES MF membranes

Ag NPs containing PES MF membranes were prepared according to our previous work [38]. Briefly, dry membrane coupons were immersed in isopropanol water solution (25%) for 30 min, followed by 3 cycles of wash using DI water (1 h for each cycle). The pre-wetted membrane coupons were immersed in dopamine solution (2 mg mL^{-1}, Tris–HCl 10 mM, pH 8.5) for 1 h, and then thoroughly rinsed with DI water to remove loosely bonded polydopamine. Then, the polydopamine coated membrane coupons were immersed in the silver nitrate solution (50 mM) for 2 h. The silver ions were reduced by the catechol groups of polydopamine to form Ag NPs on membrane surface. Finally, the Ag NPs generated membrane coupons were rinsed with DI water and air-dried for further characterization.

Membrane characterization

The membrane surface morphology was observed using by a field emission scanning electron microscopy (SEM, S-4800, Hitachi, Japan). The membrane surface elements were detected using EX-350 Energy Dispersive X-ray Microanalyzer (EDX, Horiba, Tokyo, Japan). All SEM samples were sputter-coated with platinum to provide an electrically conductive surface. The membrane hydrophilicity was determined by conducting contact angle measurement using an optical instrument (OCA 20, Data Physics, Germany). After dropping a 2 μL DI water on the membrane surface for 1 s, the shape of the droplet was recorded and analyzed using software (SCA20, version 2). The membrane samples were dried at 60 °C for 12 h and the test temperature was maintained at 25 °C.

Antibacterial tests

The diffusion inhibition zone (DIZ) test and colony-forming count (CFU) test were used to evaluate the antibacterial properties of membrane following our previous protocol [40,44]. The *E. coli* (DH5α) was used as a model microorganism. The PES MF membranes were punched into circular coupons with a diameter of 1.6 cm and sterilized by ultraviolet irradiation for 30 min. For the DIZ test, *E. coli* cells were cultured in LB broth overnight and 100 μL of the bacterial solution was spread onto LB agar plates. Then, the sterilized membrane coupons were put on the agar plates and incubated at 37 °C overnight. The inhibition zone formed around the membrane coupons was observed and photographed. For the CFU test, 1 mL overnight culture of *E. coli* was seeded into 24 mL fresh liquid LB broth and cultured for 4 h to reach the exponential growth phase of bacteria. Subsequently, the bacteria cells were harvested through centrifugation and then resuspended using physiological saline solution (containing 0.15 M NaCl, 20 mM $NaHCO_3$, pH 7.0) to achieve a cell density of 1.0×10^7 CFU mL^{-1}. The sterilized membrane coupons were placed into glass vials with 10 mL *E. coli* suspension and incubated in a shaking incubator at 37 °C for 5 h. After that, the membrane coupons were put into 10 mL physiological saline solution, followed by 7 min bath sonication to remove the bacteria from membrane surface. The bacteria solutions were serially diluted and plated onto LB agar plates. The bacteria colonies were counted after 24 h incubation at 37 °C.

The bacteria attached on membrane surface were further characterized using a live/dead stain assay. The sterilized membrane coupons were immersed in 20 mL LB broth with a cell

density of 1.0×10^7 CFU mL^{-1}. After 24 h incubation at 37 °C, the membrane coupons were rinsed with physiological saline solution and stained using SYTO®9 (3.34 μM) and PI (20 μM) for 15 min, respectively. Finally, the membrane coupons were rinsed with DI water and observed using a confocal laser scanning microscopy (CLSM, FV1000, Olympus, Japan).

The performances of Ag NPs containing PES MF membranes in a cross-flow filtration system during the fermentation broth concentration

The Ag NPs containing PES MF membranes were used to concentrate a fermentation broth in a cross-flow filtration set-up. A monoculture of *E. coli* in LB liquid broth with OD_{600} 0.6 ($\sim 10^{14}$ CFU mL^{-1}) was used as a model fermentation broth. The membrane coupon was supported by a spacer and loaded in a cell with an active membrane area of 8 cm^2. Two gear pumps were used to maintain the cross-flow velocities of 500 mL min^{-1}. The pressure was manually adjusted to 1.0 bar using a pressure valve and monitored with a pressure gauge. The initial volume of feed solution was 1 L. The real-time permeate flux was determined by measuring the weight change of the feed solution using an electronic balance. The filtration operation was conducted for 120 min, followed by 10 min back-washing with 100 mL of DI water permeate through the membrane. Another two filtration and backwashing cycles were performed to observe the water flux decline and flux recovery.

Cake layer characterization

The cake layer formed on the membrane surface was analyzed using CLSM. A membrane coupon with 1 cm^2 surface area was cut from the fouled membrane after taken out from the filtration cell, and gently rinsed with physiological saline solution and then stained by SYTO®9. Unbound stain was removed by rinsing the samples three times with sterile physiological saline solution. The fluorescence images of cake layer were obtained through a Z stack scan using CLSM. The thickness of the slice was set to 1.0 μm. The three dimensional images of cake layer were reconstructed using a software (Fluo View FV1000 Viewer, Version.2.1c). The thickness of cake layer was obtained by counting the number of slices.

Bacterial activity analysis

The activity of bacteria in the fermentation broth was analyzed using a live/dead stain assay and a growth curve method. At the end of the filtration operation, 100 μL fermentation solution was taken and mixed with 10 μL SYTO®9 (3.34 μM) and 10 μL PI (20 μM) to stain live and dead cells, respectively. Then, the *E. coli* cells in the solution were observed using a fluorescent microscope (IX81, Olympus, Japan). To obtain the growth curve of *E. coli*, 1 mL fermentation broth was added into 150 mL fresh LB liquid broth and incubated at 37 °C under 200 rpm shaking. Every 30 min, the OD_{600} of the fermentation solution was measured using a UV–vis spectrometer (TU-1810, Persee, China) to monitor the bacteria growth.

Silver leaching test

To evaluate the silver release from the Ag NPs modified membranes, 3.85 cm^2 coupons of the Ag NPs modified membrane were placed in a filtration cell (Amicon 8010, Milipore) and tested using DI water as a feed solution under the pressure of 0.1 bar. At different time intervals, the permeated solution was collected and digested with 3.5% HNO_3. Subsequently, the silver ions in the samples were analyzed using an inductively coupled plasma mass spectrometry (ICP-MS, ELAN DRC II, PerkinElmer (Hong Kong) Ltd.). The total amount of Ag NPs loaded on the PES MF membrane was determined by immersing the membrane coupons with 2 cm^2 surface area into 3.5% HNO_3 solution for 48 h. The concertation of silver ions in the solutions was measured using ICP-MS.

Results and discussion

Surface morphology and water permeability of Ag NPs containing PES MF membrane

The Ag NPs containing PES MF membranes were prepared through two steps including the PDA coating and subsequential growth of Ag NPs following our previous work [38]. The surface morphology of membranes was observed by SEM. As shown in Fig. 1, the pristine PES membrane showed a characteristic smooth surface with large cellular pores in micron size. The PDA coating presented aggregates on the membrane surface [45,46]. After the generation of Ag NPs, nanoparticles about 30 nm in average diameter were densely populated as bright dots on the membrane surface. The chemical elemental composition analysis determined by EDX reveals that the Ag NPs generated PES membrane had strong signals of silver, confirming the successful generation of Ag NPs on membrane surface. It is reported that the electrons released during the oxidation of catechol to quinone can reduce silver ions to form Ag NPs in the solution phase, and, meanwhile the O- and N-based ligand sites from PDA serve as anchors for the binding of Ag NPs on the membrane surface [47,48]. Notably, the PDA and Ag NPs did not obviously block membrane pores.

The impact of PDA and Ag NPs generation on the water permeability of PES MF membrane was investigated in a dead-end filtration system. Fig. 2A shows that the pure water fluxes of the pristine membrane, PDA coated membrane and Ag NPs containing membrane were 20, 487.5 ± 2, 687.5 LMH, 21, 210.2 ± 2, 422.0 LMH and 21, 918.4 ± 1, 138.2 LMH, respectively, confirming that the PDA and Ag NPs have negligible influence on the permeability of PES MF membrane. Generally, the PDA deposition and Ag NPs generation may block membrane pore and increase water transport resistance, which affect more towards the membranes with small pores than the membranes with large pores [49,50]. The average pore size of the PES MF membrane was 0.22 μm, which is much larger than the scales of Ag NPs. Thus, there was no obvious change in the pore size and water permeability of the PES MF membrane. The membrane hydrophilicity was also investigated by testing the water contact angles. As shown in Fig. 2B, PDA deposition decreased the water contact angles slightly from 53.4 ± 1.2° to 48.3 ± 1.7° and Ag NPs further decreased the water contact angles to 40.1 ± 1.5°, imparting their hydrophilicity to the membrane surface. Therefore, it can conclude that the Ag NPs generation on the PES MF membrane improved the membrane hydrophilicity without impairing membrane pore size or water permeability.

Antimicrobial properties of Ag NPs containing PES MF membrane

The diffusion inhibition zone (DIZ) test and colony-forming count (CFU) test were used to evaluate the antibacterial properties of Ag NPs containing PES MF membrane. Fig. 3A shows that the bacterial-free area was clearly observed around the Ag NPs containing membrane, demonstrating the excellent diffusible antibacterial property of Ag NPs containing membrane. In comparison, there were no bacterial-free zone observed around the pristine and PDA coated membranes. Moreover, the number of live *E. coli* cells on the membrane surface was measured to quantify the antibacterial performance. As shown in Fig. 3B, 600 ± 45 CFUs were observed on the pristine membrane, while only 8 ± 3 CFUs were found on the Ag NPs containing membrane, indicating 98.8% bactericidal efficacy of Ag NPs containing membrane. Additionally,

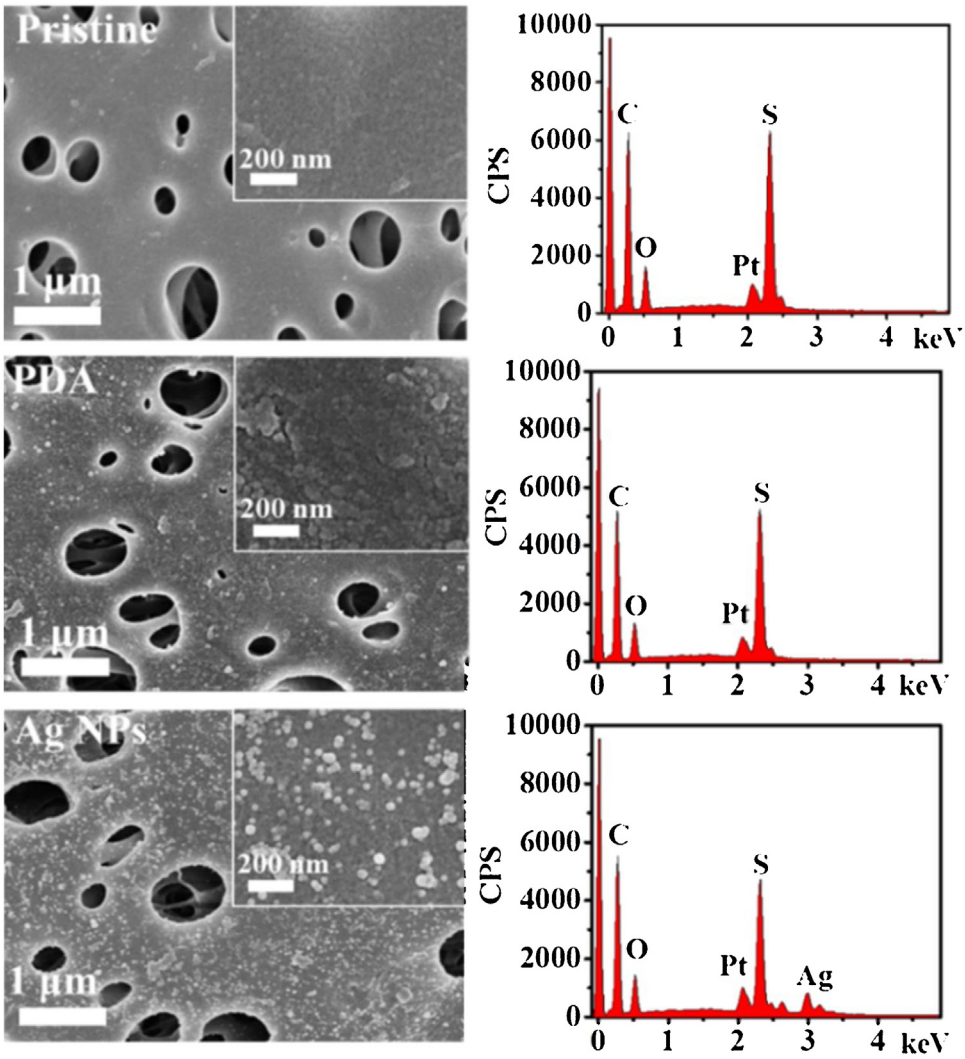

Fig. 1. SEM images and the corresponding EDX spectra of the pristine membrane, PDA coated membrane and Ag NPs containing membrane.

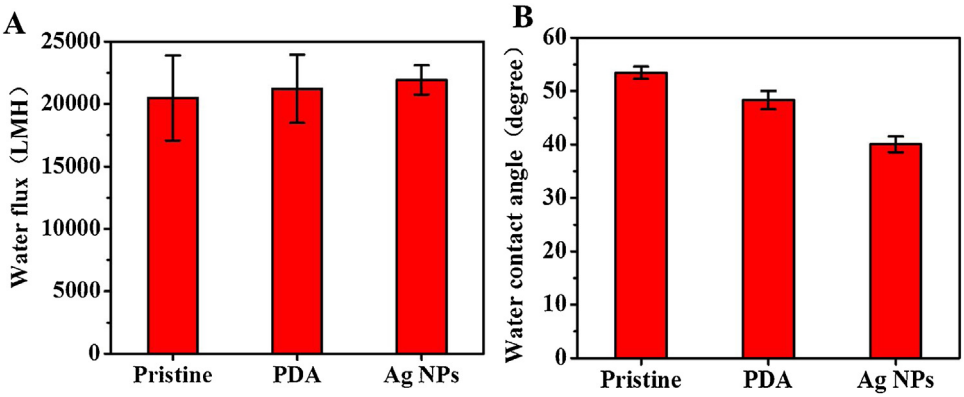

Fig. 2. The pure water fluxes (A) and contact angles (B) of the pristine membrane, PDA coated membrane and Ag NPs containing membrane.

CFUs for the PDA coated membrane decreased to 385 ± 54 compared with the pristine membrane, which may be attributed to the anti-adhesion and antibacterial properties of PDA [39].

Furthermore, the biofilm formed on the membrane surface was observed using CLSM, and the live and dead bacteria cells were stained and labeled as green and red, respectively. As shown in Fig. 3C, the pristine membrane surface was covered by a dense biofilm with populated bacteria, which was mainly composed of viable cells. Compared to the pristine, the biofilm formed on the surface of PDA coated membrane and Ag NPs containing membrane was much sparse with very few bacteria. The viable cells were predominant with a few dead cells on the surface of PDA coated

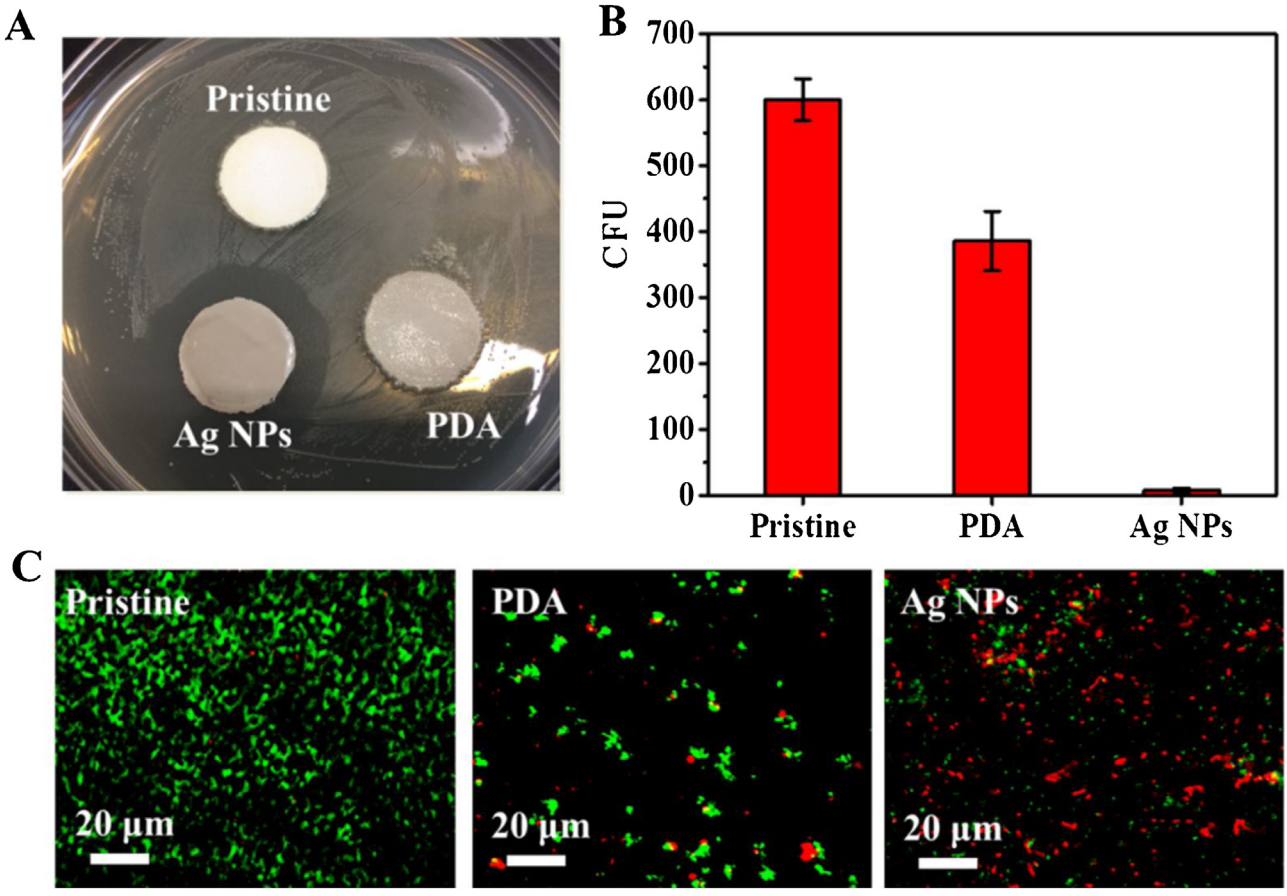

Fig. 3. Antibacterial properties of the pristine membrane, PDA coated membrane and Ag NPs containing membrane. (A) the diffusion inhibition zone images, (B) numbers of live *E. coli* cells on the membrane surface, and (C) CLSM images of representative biofilm on membrane surfaces after 24 h incubation with bacteria. Dead and live cells were stained with PI (red) and SYTO® 9 (green), respectively. (For interpretation of the references to color in this figure legend, the reader is referred to the web version of this article.)

membrane, further confirming the anti-adhesion and antibacterial properties of PDA. The dead cells were predominant with very few live cells on the surface of Ag NPs containing membrane, proving the strong antibacterial performance of Ag NPs.

The biofouling mitigation performance and mechanism of Ag NPs containing PES MF membrane during the fermentation broth concentration

The water flux of PES MF membranes was monitored in a cross-flow filtration system during the fermentation broth concentration. Physical backwashing was periodically performed to recover the membrane flux via removing the bacteria cake layer formed on membrane surface. As shown in Fig. 4, a rapid flux decline occurred to all of the PES MF membranes, indicating all membranes suffered severe membrane fouling. During the filtration operation, the water flux of Ag NPs containing membrane declined by 81.3%, very close to 81.1% for the PDA coated membrane but slightly less than 87.2% for the pristine membrane. After the physical backwash cleaning, 96.2% of the water flux for Ag NPs containing membrane was recovered, significantly higher than 83.7% and 69.8% for the corresponding PDA coated membrane and pristine membrane, suggesting that silver nanoparticles on the membrane surface facilitate the effective removal of cake layer and thus enhance water flux recovery. During the second filtration cycle, 81.4% of water flux decline for the Ag NPs containing membrane was observed, similar as 81.2% for the PDA coated membrane but less than 87.4% of the pristine membrane. All membranes exhibited very similar flux decline phenomenon during the second filtration cycle as the first cycle, which further proved that the Ag NPs modified membrane could mitigate biofouling to a limited extent during the filtration process, similar as the PDA coated membrane. Upon the second cleaning operation, 77.0% of water flux was

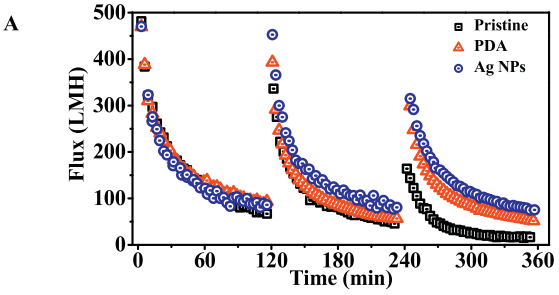

B

Cycle	Reversible fouling (%)			Irreversible fouling (%)		
	Pristine	PDA	Ag NPs	Pristine	PDA	Ag NPs
1	69.8	83.7	96.2	30.2	16.3	3.8
2	45.9	57.4	77.0	54.1	42.6	23

Fig. 4. The flux profile of the pristine membrane, PDA coated membrane and Ag NPs containing membrane during the filtration process of *E. coli* concentrate solution and after the backwash cleaning process. The reversible fouling was calculated as $R_r = (J_r/J_o) \times 100\%$, where J_r is a recovered water flux after cleaning and J_0 is an initial water flux, and the irreversible fouling was calculated as $R_{ir} = (1 - R_r) \times 100\%$. The monoculture of *E. coli* in LB broth with OD_{600} of 0.6 (10^{14} CFU mL^{-1}) was used as a feed solution. The filtration process was operated at 1.0 bar for 120 min, followed by 10 min back-washing with 100 mL DI water permeate through.

recovered for the Ag NPs containing membrane, obviously higher than 57.4% and 45.9% for the corresponding PDA coated membrane and pristine membrane. These results further demonstrate that the advantage of Ag NPs containing membrane is to facilitate the cake layer removal during the cleaning process and thus to enhance the water flux recovery through the cleaning operation. It is worthy to mention that the water flux decline of the PDA coated membrane was slower than that of the pristine membrane during the third filtration cycle, which might be attributed to the anti-adhesive properties of the PDA coating. Additionally, during the third filtration cycle, the water flux of Ag NPs containing membrane was 75.6 LMH, higher than 53.0 LMH and 16.5 LMH for the corresponding PDA coated membrane and pristine membrane. Fig. 4B shows the reversible fouling and irreversible fouling of all three different membranes to find their reversible fouling decrease and irreversible fouling increase with the increasing cycle of test, which may be ascribed to the accumulative biofouling effect from the unremovable biofilm. The Ag NPs containing membrane exhibited a higher percentage of reversible fouling and a lower percentage of irreversible fouling than that of the PDA coated membrane and pristine membrane. In the long-term run, the Ag NPs containing membrane would be expected to show distinctive advantages of maintaining high water flux and gaining high flux recovery via the physical cleaning process. In addition, the PDA coated membrane also presented good biofouling mitigation performance in comparison with the pristine membrane.

To understand the biofouling mitigation mechanisms of Ag NPs containing membrane, the cake layer formed on membrane surface was stained and analyzed using CLSM. As shown in Fig. 5, the surfaces of the pristine membrane, PDA coated membrane and Ag NPs containing membrane were completely masked by dense bacteria cakes after three cycles of filtration, which resulted in serious flux decline for all three types of membranes with little distinguishable difference. It is because that, the foulant-foulant interaction rather than the foulant-membrane interaction was the dominant factor for membrane fouling under these severe fouling conditions. The bacteria would mask the membrane surface rapidly and the membrane surface properties had negligible effect on the bacteria deposition [11,43,51]. Therefore, the Ag NPs and PDA exhibited little biofouling mitigation performance during the first filtration cycle. While, more dead cells were observed on the Ag NPs containing membrane surface than that on the pristine and PDA coated membrane surfaces (Fig. 5G, H and I). After three cycles of the filtration and physical backwash cleaning operation, the bacteria cakes were partially washed off from the membrane surface, and the thickness of cake layer for the Ag NPs generated membrane and PDA coated membrane decreased from 8 μm to 6 μm, significantly lower than 14 μm of the pristine membrane. Noticeably, the bacteria attached on Ag NPs containing membrane and PDA coated membrane were much less and sparse than that on the pristine membrane upon the cleaning. The aforementioned results has

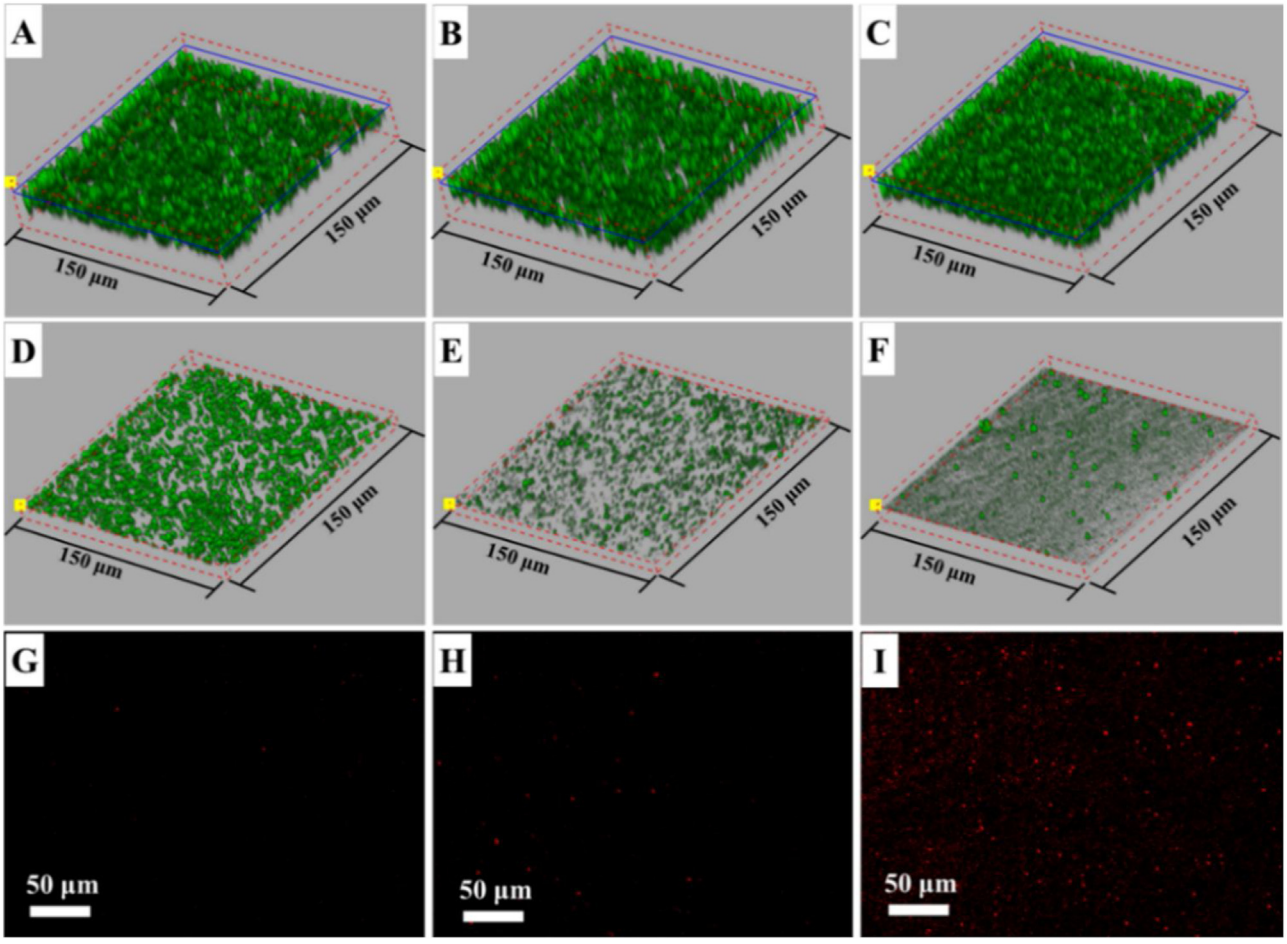

Fig. 5. The CLSM 3-D images of the cake layer formed on the pristine membrane, PDA coated membrane and Ag NPs containing membrane after three cycles of filtration (A, B and C) and cleaning processes (D, E and F). Bacteria cells were stained with SYTO® 9. Representative CLSM images of dead cells on the surface of the pristine membrane, PDA coated membrane and Ag NPs containing membrane after three cycles of filtration (G, H and I without cleaning operation, same samples from A, B and C). Bacteria cells were stained with PI.

proved that the PDA has anti-adhesive property and Ag NPs could kill bacteria efficiently. Therefore, the biofouling mitigation mechanism of the PDA and Ag NPs on the PES membrane surfaces is mainly because of the effective removal of bacteria cake layer from the modified membrane surface.

For the real fermentation broth filtration, the interactions between foulants and the membrane surfaces are much more complex. The pH of the solution may play an important role to affect the foulant–membrane interactions, since it can affect the association-dissociation of fermentation broth components and thus influence the adsorption of foulants on membrane surfaces [52]. Generally, bacterial cells in fermentation broth aggregate at a low pH because the cell–cell electrostatic interactions are less repulsive and hydrophobic forces are weak at a low pH, which results in a loose cake layer and low resistance [53]. Moreover, the bacteria cell, broth medium, proteins and other metabolic products of bacteria have different fouling behaviors on the membrane surface during the filtration, and thus membrane fouling is a combined fouling of fermentation broth compositions [8]. It deserves a comprehensive investigation to concentrate a real fermentation broth in the future.

Silver leaching from membrane surface and the impacts of silver on bacterial activity in the fermentation broth

The silver ions release profiles illustrate that Ag NPs exhibited a slow and steady release behavior as shown in Fig. 6. The silver concentration in the permeate was between 0.2 $\mu g\,L^{-1}$ and 0.3 $\mu g\,L^{-1}$, which were an order of magnitude lower than the maximal contaminant limit of silver in drinking water (0.1 $mg\,L^{-1}$) according to the World Health Organization [54]. The silver loading amount of Ag NPs containing membrane was measured to be $17.4 \pm 4.9\ \mu g/cm^2$. During the 24 h filtration test, the accumulated silver ions amount was 1.9 μg, which was only 3.3% of its original silver loading mass. Our previous work also proved that Ag NPs generated on the membrane surface through the PDA coating released very slowly in a long-term test [38]. Therefore, the Ag NPs were very stable and released slowly from the membrane surface.

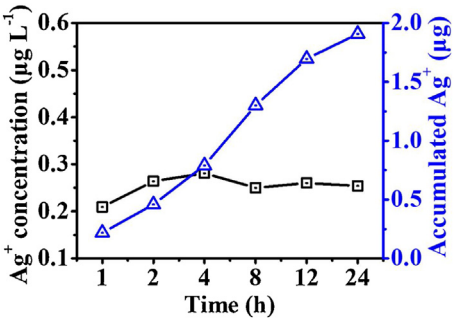

Fig. 6. The silver ions release curves from the Ag NPs containing membrane during 24 h filtration operation. DI water was continuously filtered through the Ag NPs containing membranes in a dead-end filtration cell under the pressure of 0.1 bar.

To study the impact of Ag NPs on bacterial activity in the fermentation broth, the live/dead stain assay and growth curve method were employed to examine the activity of *E. coli* in the concentrated fermentation broth. As shown in Fig. 7A, the

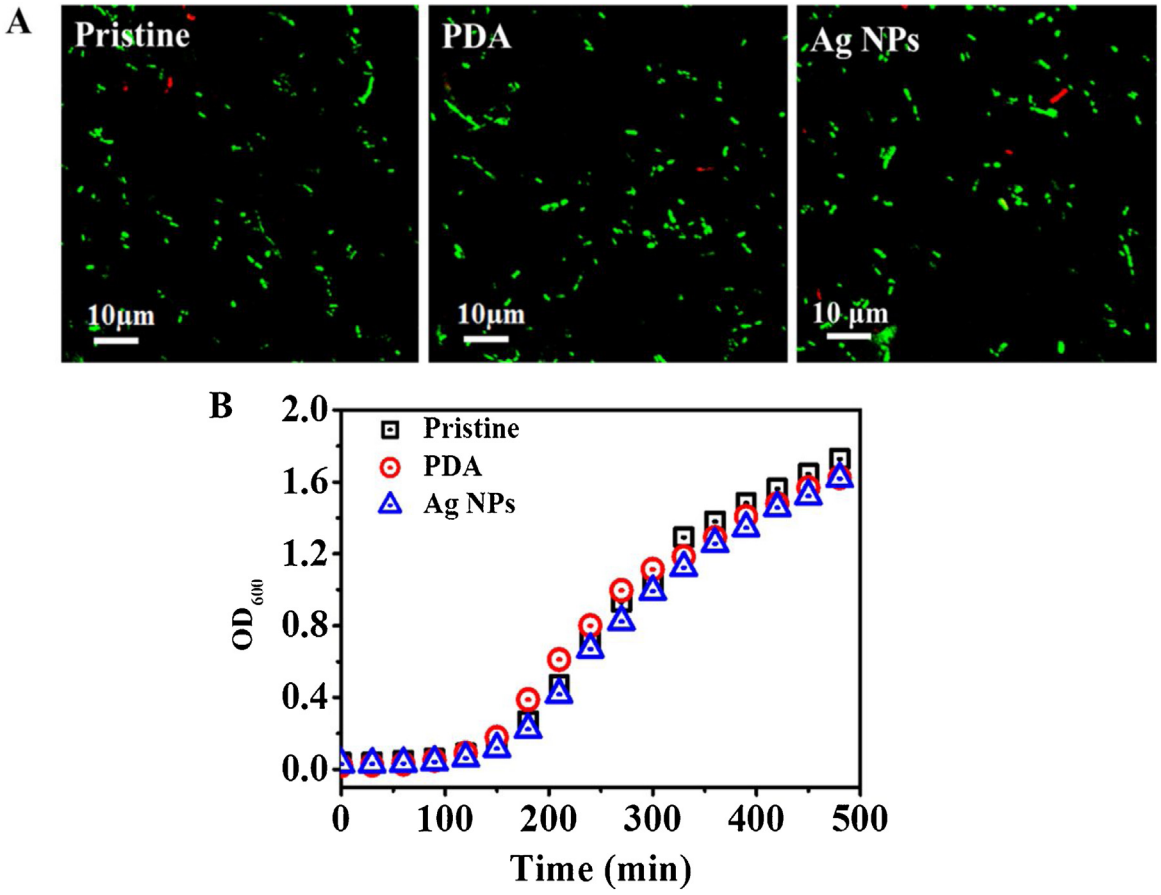

Fig. 7. Representative fluorescence microscope images and growth curves of *E. coli* taken from the concentrated feed solution after the concentration process using the pristine membrane, PDA coated membrane and Ag NPs containing membrane respectively. (For interpretation of the references to color in the text, the reader is referred to the web version of this article.)

green fluorescence was predominant in the images from bacteria taken from the concentrated fermentation broth through the filtration process using the pristine membrane, PDA coated membrane and Ag NPs containing membrane, and no obvious difference of red fluorescence was observed. These results illustrate that the bacterial activity was not affected by the concentration process using the Ag NPs containing membrane. Fig. 7B shows the growth curves of *E. coli.* A typical lag phase from 0 to 100 min and an exponential phase from 100 to 480 min were observed for *E. coli.* upon concentration using all of the three types of membranes. No growth inhibition of bacteria was observed from the sample after the concentration using the Ag NPs containing membrane, which may because of super low amount of silver ions released from the membrane. All these results demonstrate that the Ag NPs containing membrane has no negative effect on the bacterial activity and shows a great application potential in the concentration process of fermentation broth.

Conclusions

In this study, we fabricated the Ag NPs containing PES MF membrane to concentrate bacteria cells from fermentation broth, and investigated its biofouling mitigation performance and mechanism under severe fouling conditions using a high concentration of *E. coli* solution as a simulative fermentation broth. During each filtration process, the Ag NPs containing membrane did not present any significant biofouling mitigation performances, because the foulant–foulant interaction rather than the foulant–membrane interaction was the dominant factor to foul membrane surfaces and the membrane surface properties had negligible effect on the bacteria deposition under the severe fouling conditions. But, importantly, after each cycle of physical cleaning, the Ag NPs containing membrane presented distinctive higher water flux and slower flux decline compared with the pristine membrane and the PDA coated membrane. The cake layer analysis further illustrated that the bacteria attached on membrane surface were deactivated by Ag NPs and could be removed efficiently during the backwash cleaning process. Therefore, the biofouling mitigation mechanism of the Ag NPs containing membrane was to make the bacteria cake layer remove efficiently, and thus to suppress the biofilm development on the membrane surface in the long-term run. Moreover, the Ag NPs on the membrane surface released very slowly and has no negative impact on the activities of bacteria in the concentrated fermentation broth. Our study provides new insights into the biofouling mitigation performances and mechanisms of the antibacterial membrane under the conditions of high fouling tendency, and the application potential of the antibacterial membrane for the fermentation broth treatment.

Competing interest

The authors declare no competing financial interest.

Acknowledgements

The authors gratefully acknowledge the funding support from National Natural Science Foundation of China (Nos. 21476249, 51708408), Chang-jiang Scholars and Innovative Research Team in the University of Ministry of Education, China (No. IRT-17R80), Program for Innovative Research Team in University of Tianjin (No. TD13-5044) and the Science and Technology Plans of Tianjin (No. 17PTSYJC00060).

References

[1] K. Keller, T. Friedmann, A. Boxman, Trends Biotechnol. 19 (2001) 438.
[2] B. Wojciech, E. Celińska, R. Dembczyński, D. Szymanowska, M. Nowacka, T. Jesionowski, W. Grajek, J. Membr. Sci. 427 (2013) 118.
[3] M.H.M. Isa, D.E. Coraglia, R.A. Frazier, P. Jauregi, J. Membr. Sci. 296 (2007) 51.
[4] X. Yang, S. Zhou, M. Li, R. Wang, Y. Zhao, Sep. Purif. Technol. 175 (2017) 435.
[5] Y. Wang, H. Meng, D. Cai, B. Wang, P. Qin, Z. Wang, T. Tan, Bioresour. Technol. 211 (2016) 291.
[6] H. Liu, Y. Wang, B. Yin, Y. Zhu, B. Fu, H. Liu, Bioresour. Technol. 218 (2016) 92.
[7] M. Waszak, M. Gryta, Chem. Eng. J. 305 (2016) 129.
[8] E. Kujundzic, A.R. Greenberg, R. Fong, B. Moore, D. Kujundzic, M. Hernandez, J. Membr. Sci. 349 (2010) 44.
[9] C. Harscoat, M.Y. Jaffrin, R. Bouzerar, J. Courtois, Biotechnol. Bioeng. 65 (2015) 500.
[10] R.S. Juang, H.L. Chen, Y.S. Chen, Sep. Purif. Technol. 63 (2008) 531.
[11] C. Wang, Q. Li, H. Tang, D. Yan, W. Zhou, J. Xing, Y. Wan, Bioresour. Technol. 116 (2012) 366.
[12] D.Y. Lee, Y.Y. Li, T. Noike, G.C. Cha, J. Membr. Sci. 322 (2008) 13.
[13] S.T. Kang, A. Subramani, E.M.V. Hoek, M.A. Deshusses, M.R. Matsumoto, J. Membr. Sci. 244 (2004) 151.
[14] A.I.C. Morão, A.M.B. Alves, M.C. Costa, J.P. Cardoso, Desalination 200 (2006) 472.
[15] Y. Gao, D. Chen, L.K. Weavers, H.W. Walker, J. Membr. Sci. 401–402 (2012) 232.
[16] B.G. Park, W.G. Lee, W. Zhang, Y.K. Chang, H.N. Chang, J. Microbiol. Biotechnol. 9 (1999) 243.
[17] L. Wang, Q. Wang, Y. Li, H. Lin, Desalination 326 (2013) 103.
[18] H.L. Chen, Y.S. Chen, R.S. Juang, Sep. Purif. Technol. 62 (2008) 47.
[19] C. Xue, Z.X. Wang, G.Q. Du, L.H. Fan, Y. Mu, J.G. Ren, F.W. Bai, Process Biochem. 51 (2016) 1140.
[20] R. Zhang, Y. Liu, M. He, Y. Su, X. Zhao, M. Elimelech, Z. Jiang, Chem. Soc. Rev. 45 (2016) 5888.
[21] N. Dizge, G. Soydemir, A. Karagunduz, B. Keskinler, J. Membr. Sci. 366 (2011) 278.
[22] E. Barzeev, F. Perreault, A.P. Straub, M. Elimelech, Environ. Sci. Technol. 49 (2015) 13050.
[23] E. Arkhangelsky, D. Kuzmenko, V. Gitis, J. Membr. Sci. 305 (2007) 176.
[24] J. Mansouri, S. Harrisson, V. Chen, J. Mater. Chem. 20 (2010) 4567.
[25] N. Akar, B. Asar, N. Dizge, I. Koyuncu, J. Membr. Sci. 437 (2013) 216.
[26] H.Y. Yu, Y. Kang, Y. Liu, B. Mi, J. Membr. Sci. 449 (2014) 50.
[27] W.F. Chan, E. Marand, S.M. Martin, J. Membr. Sci. 509 (2016) 125.
[28] A.F. Faria, C. Liu, M. Xie, F. Perreault, D.N. Long, J. Ma, M. Elimelech, J. Membr. Sci. 525 (2017) 146.
[29] J. Lv, G. Zhang, H. Zhang, F. Yang, Chem. Eng. J. 352 (2018) 765.
[30] V. Vatanpour, A. Shockravi, H. Zarrabi, Z. Nikjavan, A. Javadi, J. Ind. Eng. Chem. 30 (2015) 342.
[31] B.L. Ouay, F. Stellacci, Nano Today 10 (2015) 339.
[32] J. Dolina, O. Dlask, T. Lederer, L. Dvořák, Chem. Eng. J. 275 (2015) 125.
[33] E. Koh, Y.T. Lee, J. Ind. Eng. Chem. 47 (2017) 260.
[34] K. Zodrow, L. Brunet, S. Mahendra, D. Li, A. Zhang, Q. Li, P.J. Alvarez, Water Res. 43 (2009) 715.
[35] X. Liu, L.X. Foo, Y. Li, J.Y. Lee, B. Cao, C.Y. Tang, Desalination 389 (2016) 137.
[36] Z. Liu, L. Qi, X. An, C. Liu, Y. Hu, ACS Appl. Mater. Interfaces 9 (2017) 40987.
[37] J. Yin, Y. Yang, Z. Hu, B. Deng, J. Membr. Sci. 441 (2013) 73.
[38] Z. Liu, Y. Hu, ACS Appl. Mater. Interfaces 8 (2016) 21666.
[39] L. Qi, Y. Hu, Z. Liu, X. An, E. Bar-Zeev, Environ. Sci. Technol. 52 (2018) 9684.
[40] L. Qi, Z. Liu, N. Wang, Y. Hu, Appl.Surf. Sci. 456 (2018) 95.
[41] H. Karkhanechi, R. Takagi, H. Matsuyama, Desalination 336 (2014) 87.
[42] F. Razi, I. Sawada, Y. Ohmukai, T. Maruyama, H. Matsuyama, J. Membr. Sci. 401–402 (2012) 292.
[43] Q. She, R. Wang, A.G. Fane, C.Y. Tang, J. Membr. Sci. 499 (2016) 201.
[44] Z. Liu, Y. Hu, C. Liu, Z. Zhou, Chem. Commun. 52 (2016) 12245.
[45] Y. Li, Y. Su, J. Li, X. Zhao, R. Zhang, X. Fan, J. Zhu, Y. Ma, Y. Liu, Z. Jiang, J. Membr. Sci. 476 (2015) 10.
[46] J. Zhao, Y. Su, X. He, X. Zhao, Y. Li, R. Zhang, Z. Jiang, J. Membr. Sci. 465 (2014) 41.
[47] H. Seonki, L. Joon Seok, R. Jungki, L. Sahng Ha, L.D. Yun, K. Dong-Pyo, P.C. Beum, L. Haeshin, Nanotechnology 22 (2011) 494020.
[48] S. Murphy, L. Huang, P.V. Kamat, J. Phys. Chem. C 115 (2011) 22761.
[49] B.D. Mccloskey, H.B. Park, H. Ju, B.W. Rowe, D.J. Miller, B.J. Chun, K. Kin, B.D. Freeman, Polymer 51 (2010) 3472.
[50] B.B. Jiang, X.F. Sun, L. Wang, S.Y. Wang, R.D. Liu, S.G. Wang, Chem. Eng. J. 311 (2016) 135.
[51] D.M. Krstić, S.L. Markov, M.N. Tekić, Biochem. Eng. J. 9 (2001) 103.
[52] J. Brinck, A.S. Jönsson, B. Jönsson, J. Lindau, J. Membr. Sci. 164 (2000) 187.
[53] K. Ohmori, C.E. Glatz, J. Membr. Sci. 153 (1999) 23.
[54] H.T. Ratte, Environ. Toxicol. Chem. 18 (2010) 89.